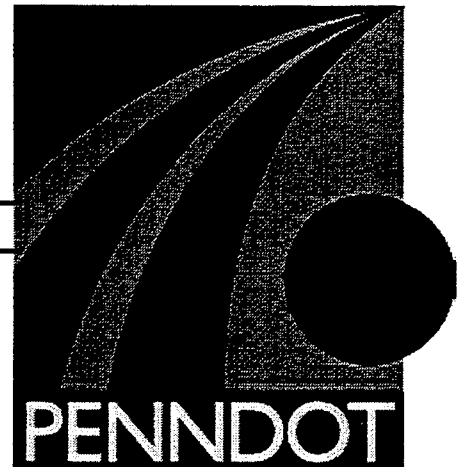




**COMMONWEALTH OF PENNSYLVANIA
DEPARTMENT OF TRANSPORTATION**

PENNDOT RESEARCH



**FIELD TESTING AND EVALUATION
OF LAUREL HILL CREEK BRIDGE**

**University-Based Research, Education,
and Technology Transfer Program**

AGREEMENT NO. 359704, WORK ORDER 11

FINAL REPORT

February 2002

By H. Gangarao, V. Shekar, and K. Lasiophriang

PENNSSTATE



Pennsylvania Transportation Institute

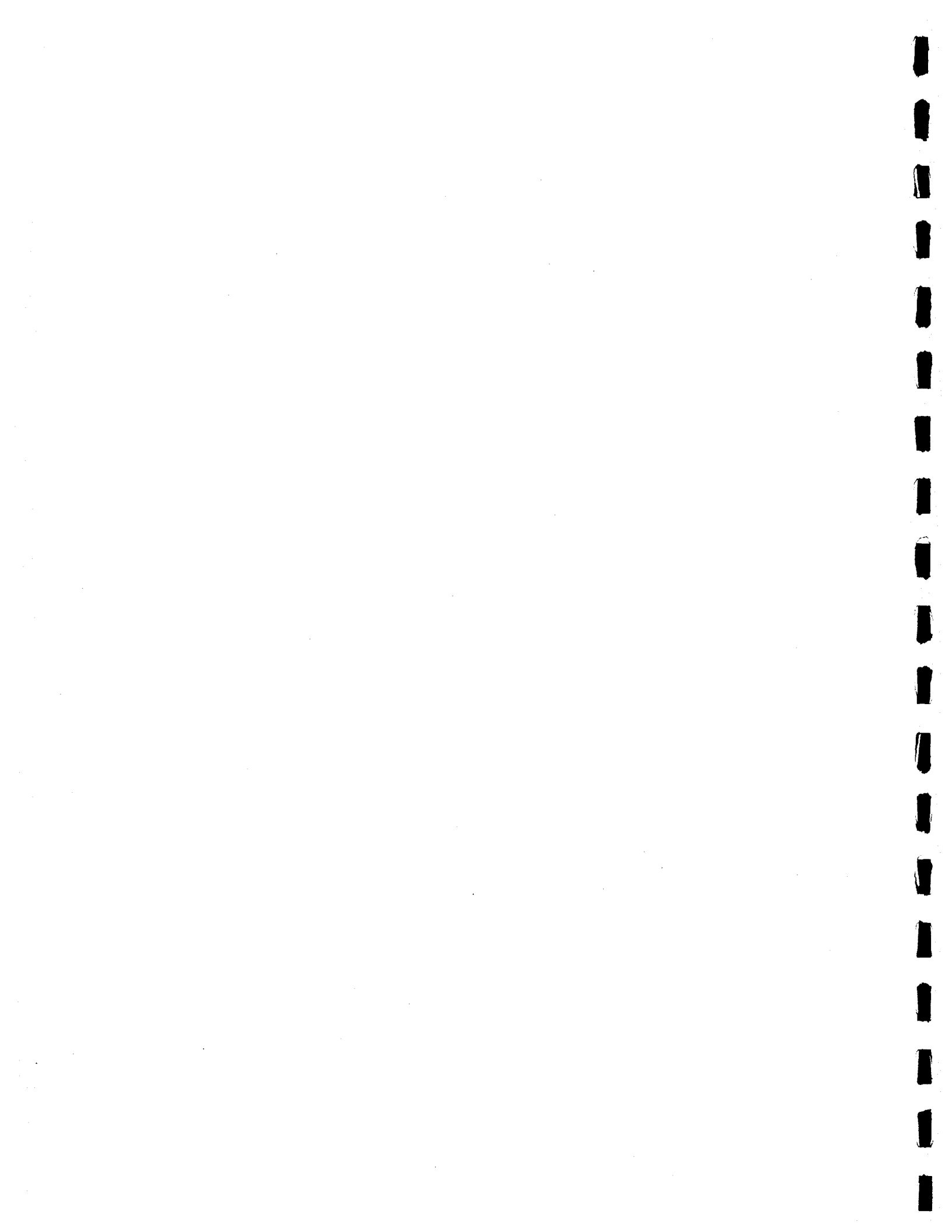
**The Pennsylvania State University
Transportation Research Building
University Park, PA 16802-4710
(814) 865-1891 www.pti.psu.edu**

Reproduced from
best available copy.

**PROTECTED UNDER INTERNATIONAL COPYRIGHT
ALL RIGHTS RESERVED
NATIONAL TECHNICAL INFORMATION SERVICE
U.S. DEPARTMENT OF COMMERCE**

REPRODUCED BY: **NTIS**
U.S. Department of Commerce
National Technical Information Service
Springfield, Virginia 22161

1. Report No. FHWA-PA-2002-006-97-04 (11)	2. Government Accession No.	3. Recipient's Catalog No.	
4. Title and Subtitles Field Testing and Evaluation of Laurel Hill Creek Bridge		5. Report Date February 18, 2002	6. Performing Organization Code
7. Authors Hota Gangarao, Vimala Shekar, and Krit Lasiophriang West Virginia University		8. Performing Organization Report No. PTI 2002-20	
9. Performing Organization Name and Address. The Pennsylvania Transportation Institute Transportation Research Building The Pennsylvania State University University Park, PA 16802		10. Work Unit No. (TRAIS)	11. Contract or Grant No. 359704, Work Order 11
12. Sponsoring Agency Name and Address The Pennsylvania Department of Transportation Bureau of Planning and Research Commonwealth Keystone Building 400 North Street, 6 th Floor Harrisburg, PA 17120		13. Type of Report and Period of Covered Final Report, 9/23/1998 – 12/23/2001	
		14. Sponsoring Agency Code	
15. Supplementary Notes CTOR: Rebecca Burns (717) 787-7506			
16. Abstract <p>Bridge deck deterioration has been recognized by highway agencies as one of the most complex problems that plagues United States transportation infrastructures (Gangarao, 1999). Federal and state transportation agencies have turned to investigating non-conventional advanced materials to help solve the deterioration problems of highway infrastructure, especially bridge decks. Fiber reinforced polymer (FRP) composites are one of the advanced materials considered to have high potential for use in bridge deck repair and replacement. Advances in manufacturing and design of FRP composites have lead to the production of bridge deck modules that can be used as temporary or permanent replacements for bridge decks (Gangarao, 1999).</p> <p>The Constructed Facilities Center of West Virginia University (CFC-WVU), in cooperation of Pennsylvania Department of Transportation (PENNDOT) constructed an FRP composite deck-steel stringer bridge (Laurel Hill Creek) in 1998 in Somerset County, Pennsylvania. Shortly after construction, CFC-WVU had initiated monitoring the in-service performance of the FRP composite deck bridge over a three-year time period.</p> <p>The FRP composite deck stiffened by steel stringers on the Laurel Hill Creek Bridge was subjected to actual truckloads, and also to real environmental loads. Thus, Laurel Hill Creek Bridge provides an excellent opportunity to evaluate its performance of bridge under static and environmental loads. This report presents several technical details on the construction and performance evaluation of Laurel Hill Creek Bridge. The performance evaluation entails: 1) load testing and evaluation of strains and deflections induced under HS-20 loading conditions; 2) degree of structural composite action between the FRP deck and steel stringers; 3) transverse load distribution factor; 4) performance of deck-to-beam connections, and 5) deck deformations.</p>			
17. Key Words Bridge deck deterioration, Laurel Hill Creek Bridge of Somerset County, Pennsylvania		18. Distribution Statement No restrictions. This document is available from the National Technical Information Service, Springfield, VA 22161	
19. Security Classif. (of this report) Unclassified	20. Security Classif. (of this page) Unclassified	21. No. of Pages	22. Price



FIELD TESTING AND EVALUATION OF LAUREL HILL CREEK BRIDGE
University-Based Research, Education, and Technology Transfer
Agreement No. 359704
Work Order 11

FINAL REPORT

Prepared for

Commonwealth of Pennsylvania
Department of Transportation

By

Hota Gangarao
Vimala Shekar
Krit Lasiophriang
West Virginia University

The Pennsylvania Transportation Institute
The Pennsylvania State University
Transportation Research Building
University Park, PA 16802-4710

February 2002

This work was sponsored by the Pennsylvania Department of Transportation and the U.S. Department of Transportation, Federal Highway Administration. The contents of this report reflect the views of the author, who is responsible for the facts and the accuracy of the data presented herein. The contents do not necessarily reflect the official views or policies of either the Federal Highway Administration, U.S. Department of Transportation, or the Commonwealth of Pennsylvania at the time of publication. This report does not constitute a standard, specification, or regulation.

PTI 2002-20



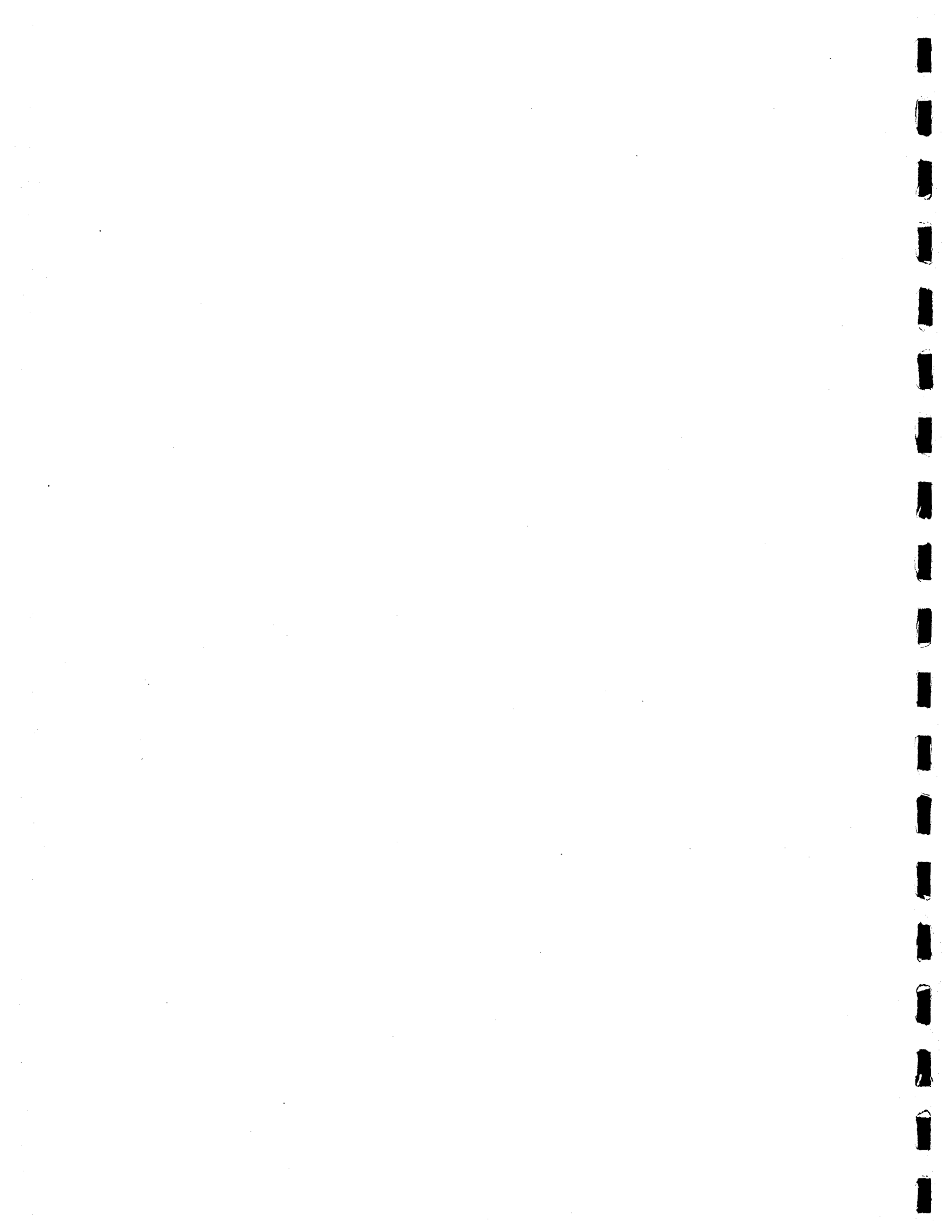
TABLE OF CONTENTS

1.0 INTRODUCTION	1
2.0 CONSTRUCTION.....	2
3.0 LOAD TESTING.....	8
4.0 INSTRUMENTATION	10
5.0 LOAD TEST RESULTS.....	12
5.1 Degree of Structural Composite Action.....	12
5.2 Transverse Load Distribution Factors.....	13
5.3 Bridge Performance	14
5.4 Deck Deformations	17
5.5 Deck-to-Beam Connections.....	17
6.0 CONCLUSIONS.....	17
7.0 RECOMMENDATION	18
8.0 REFERENCES	18
APPENDIX A.....	A-1
APPENDIX B.....	B-1



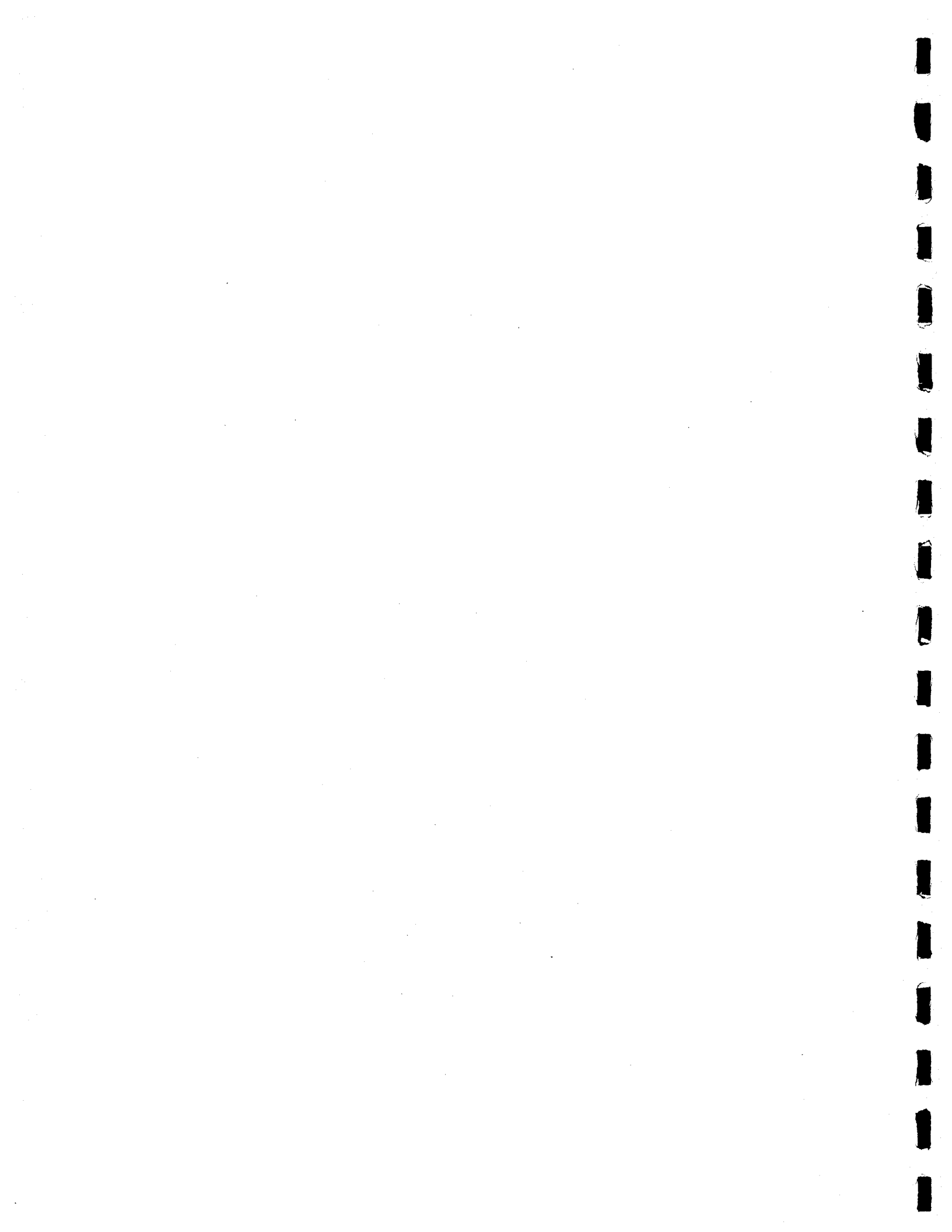
LIST OF FIGURES

Figure 1. Plan and Section of the Deck.....	3
Figure 2. Deck-to-Stringer Connection.....	4
Figure 3. Application of Adhesive at Tongue and Groove Joints.....	5
Figure 4. Abutment Details.....	7
Figure 5. Deck Edge Treatment.....	7
Figure 6. Position of Truck on One Lane	9
Figure 7. Position of Trucks on Each Lane.....	9
Figure 8. Position of Truck on One Lane Under Extreme Location.....	10
Figure 9. Location of Strain Gages on the Deck.....	11
Figure 10. Typical Strain Distributions Through the Depth of Superstructure for a Stringer.....	13



LIST OF TABLES

Table 1. Comparison of Theoretical and Experimental Transverse Load Distribution Factors.....	14
Table 2. Comparison of Theoretical and Experimental Deflections and Strains.....	16



FIELD TESTING AND EVALUATION OF LAUREL HILL CREEK BRIDGE

1.0 INTRODUCTION

Bridge deck deterioration has been recognized by highway agencies as one of the most complex problems that plagues United States transportation infrastructures (Gangarao, 1999). Federal and state transportation agencies have turned to investigating non-conventional advanced materials to help solve the deterioration problems of highway infrastructure, especially bridge decks. Fiber reinforced polymer (FRP) composites are one of the advanced materials considered to have high potential for use in bridge deck repair and replacement. Advances in manufacturing and design of FRP composites have lead to the production of bridge deck modules that can be used as temporary or permanent replacements for bridge decks (Gangarao, 1999).

The Constructed Facilities Center of West Virginia University (CFC-WVU), in cooperation of Pennsylvania Department of Transportation (PENNDOT) constructed an FRP composite deck-steel stringer bridge (Laurel Hill Creek) in 1998 in Somerset County, Pennsylvania. Shortly after construction, CFC-WVU had initiated monitoring the in-service performance of the FRP composite deck bridge over a three-year time period.

The FRP composite deck stiffened by steel stringers on the Laurel Hill Creek Bridge was subjected to actual truckloads, and also to real environmental loads. Thus, Laurel Hill Creek Bridge provides an excellent opportunity to evaluate its performance of bridge under static and environmental loads. This report presents several technical details on the construction and performance evaluation of Laurel Hill Creek Bridge. The performance evaluation entails: 1) load testing and evaluation of strains and deflections induced under HS-20 loading conditions; 2)

degree of structural composite action between the FRP deck and steel stringers; 3) transverse load distribution factor; 4) performance of deck-to-beam connections, and 5) deck deformations.

2.0 CONSTRUCTION

The Laurel Hill Creek Bridge is a single-span structure located in Jefferson Township, Somerset County, Pennsylvania. The overall length of the structure is 25' – 3 5/8" and the deck width is 25' – 6 1/2". The bridge has 90° skew with an average daily traffic of about 600 vehicles. The plan and section of the bridge are shown in figure 1.

To evaluate the viability of using FRP composite materials as an alternative for conventional materials, CFC-WVU, proposed to construct this bridge with an FRP modular deck stiffened with steel stringers, since FRP decks have several advantages over conventional decks such as:

- High strength to weight ratios
- Excellent resistance to fatigue
- Good energy absorption
- Durable
- Lighter in weight
- Ease of fabrication, handling, installation and maintenance
- Longer service

The FRP composite deck was fabricated by Creative Pultrusions, Inc. under the trade name of Superdeck™ through the pultrusion process (Lopez, 1998). The deck cross-section and the fiber architecture are designed to resist HS-25 loading. The deck cross-section consists of double trapezoid and hexagonal shapes whose fiber architectures are made of E-glass multi-axial

The FRP composite deck modules with strong bending axis, were placed transversely to span (ie., perpendicular to flow of traffic) direction and were supported by longitudinal steel stringers. The FRP deck modules (25'-6 1/2" x 8') were joined in the field using shear keys (full-depth, hexagonal components) to provide mechanical interlocking and a surface for adhesive bonding. Once the first deck module was placed on the stringers and bonded with Pliogrip and bolted with Huck bolts, the subsequent deck module was placed next to first module and the two modules were "squeezed" together to establish a good bond and full shear transfer with the remaining modules. Good bond between contiguous modules is essential to provide the in-plane force resistance. The in-plane force is primarily induced from thermal fluctuations.

The FRP deck modules were inter-connected using both adhesive bonding and mechanical fasteners (figure 2). The adhesive was applied to the tongue and groove joints (figure 3) of the first modules before the adjacent module was bonded to the first module. To allow additional curing time for the adhesive, the second module was lowered and jacked into place and a concrete barrier was placed on the top of FRP deck to achieve stability and a good bond between the deck-to-deck and deck-to-stringers (Overby, 1998). In addition to the adhesive bonding, mechanical fasteners such as blind bolts were provided in the shear keys for adequate transfer of shear between the modules.

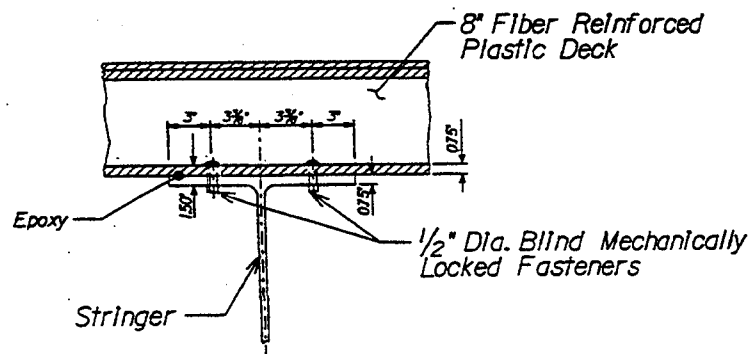


Figure 2. Deck-to-Stringer Connection.

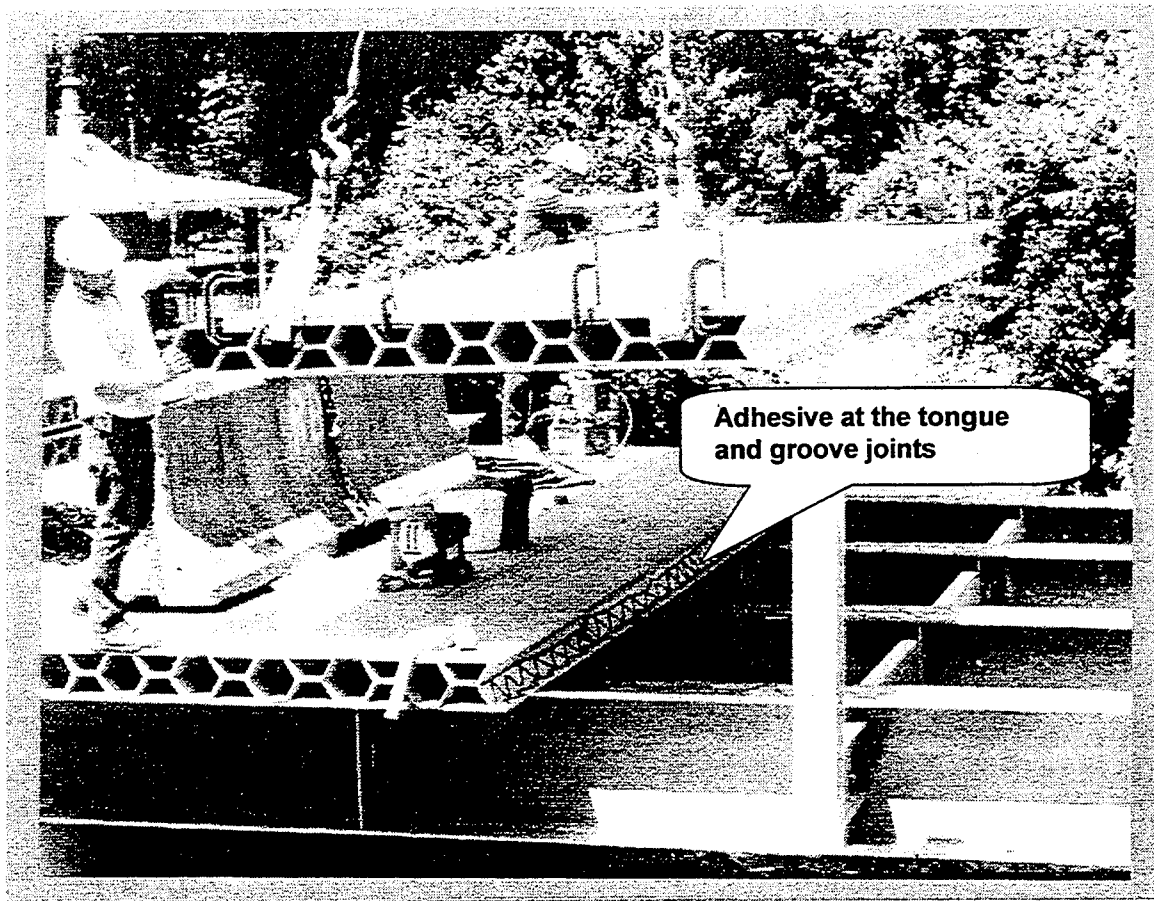


Figure 3. Application of Adhesive at Tongue and Groove Joints.

In the case of deck-stringer connections, the following steps were adopted (Lopez, 1998):

- 1) The top surface of steel stringers and bottom surface of deck were sandblasted.
- 2) The FRP deck modules were placed in position with respect to the predrilled stringers.
- 3) A primer (Pliogrip[®] 6031/6032) was applied on the top surface of steel stringers.
- 4) The stringers were covered with styrofoam sheets so as to prevent the primer from abrasion.

- 5) Primer was allowed to cure around 23 °C (73 °F) ambient temperature for about 16 to 24 hours (Note: The primer must not be placed when ambient temperature goes below 10 °C (50 °F))
- 6) Polyurethane adhesive (Pliogrip[®] 7770/300) was then applied to the primed stringer surface. The adhesive was also applied to bottom flange of deck surface and on the expansion dams.
- 7) The first deck module was aligned with stringers and was placed in position using the lifting hooks (Figure 3). A hydraulic jack was used to push the deck module against expansion dam.
- 8) The deck was then connected to the stringers using ½ in. diameter BOM[®] blind bolts from Huck International Inc. as shown in Figure 2.

In the case of guiderail connection, steel brackets were welded to the exterior stringers that were attached to guiderail posts on the FRP composite bridges. At this point, connecting the guiderail post to the FRP deck is not recommended because the guiderail connection has not been tested for crash-worthiness (The railing test level are not known).

The abutment details for the bridge are shown in figure 4. Elastomeric pads were used on the bridge seats.

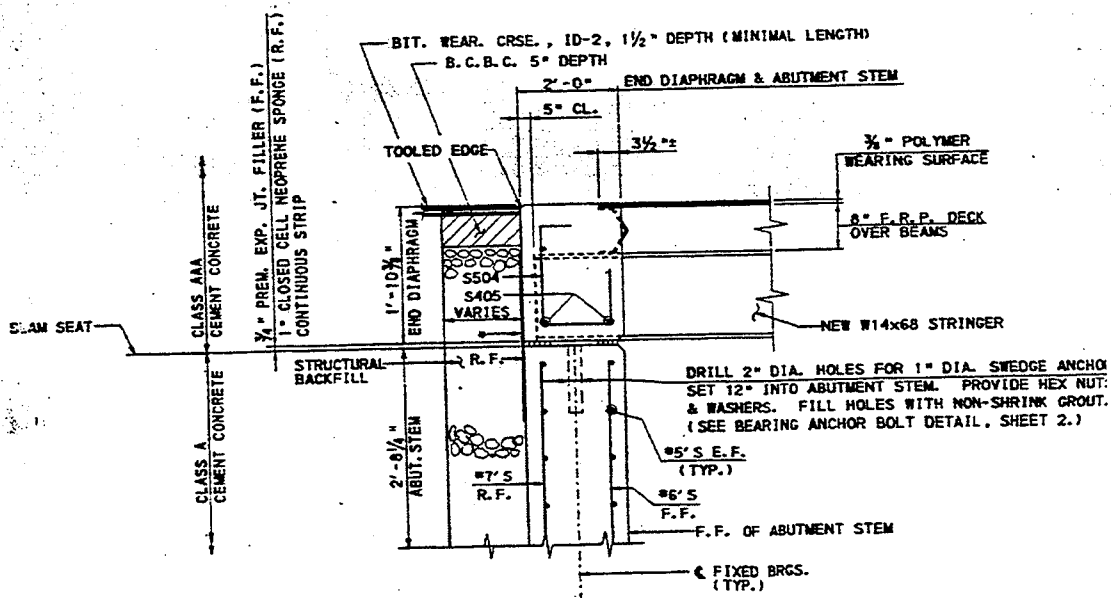


Figure 4. Abutment Details.

The open edges of FRP decks were closed with protruded angles to prevent entrance of moisture into the deck cells (Figure 5).

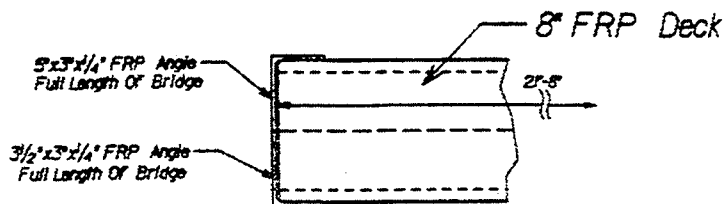


Figure 5. Deck Edge Treatment.

Once the decks were installed on the supporting stringers, a polymer concrete overlay of three-eighths of an inch thick was laid on the deck surface. The following procedure was adopted during the application of wearing surface:

- The deck surface was sandblasted.
- Polymer powder caused by surface preparation was vacuum cleaned.

- A suitable primer (urethane based) was applied.
- The Polymer Concrete (PC) was placed slowly to the required thickness.
- The PC was laid when the temperature was above 10 °C (50 °F) and below 30 °C (86 °F); otherwise, the PC may take longer than the time needed to cure for low temperature field conditions, or it may cure quicker than the time needed for proper surface screenings in case of high deck surface temperatures (GangaRao et.al, 2000).

3.0 LOAD TESTING

Three static load tests were performed on Laurel Hill Creek Bridge. The first load test was conducted in October 1998, while the second and third load tests were conducted in December 2000 and May 2001 respectively. Each of the three load tests included three load positions: 1) One loaded truck positioned in one lane - LC1 (figure 6); 2) Two loaded trucks one in each lane - LC2 (figure 7); and 3) One loaded truck positioned in the other lane - LC3 (figure 8). During the load tests, strains and deformations of stringers and the deck were recorded before and during the application of the load.

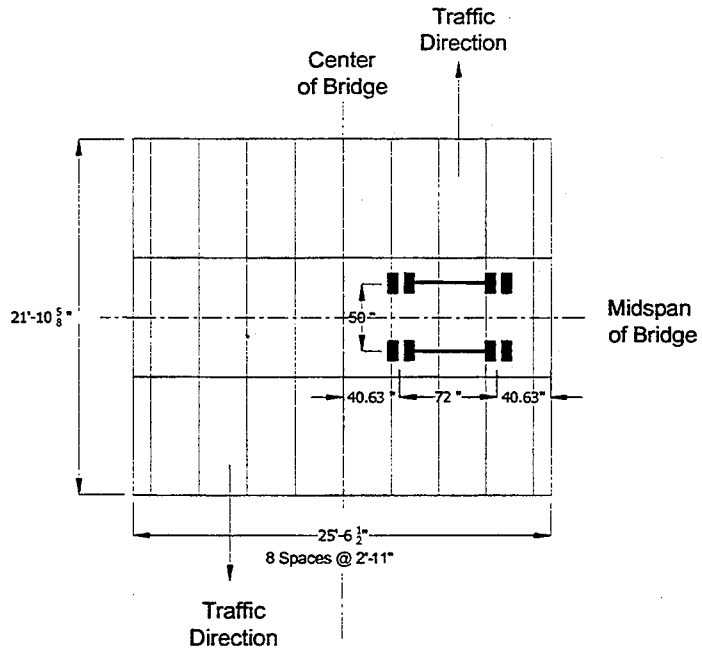


Figure 6. Position of Truck on One Lane.

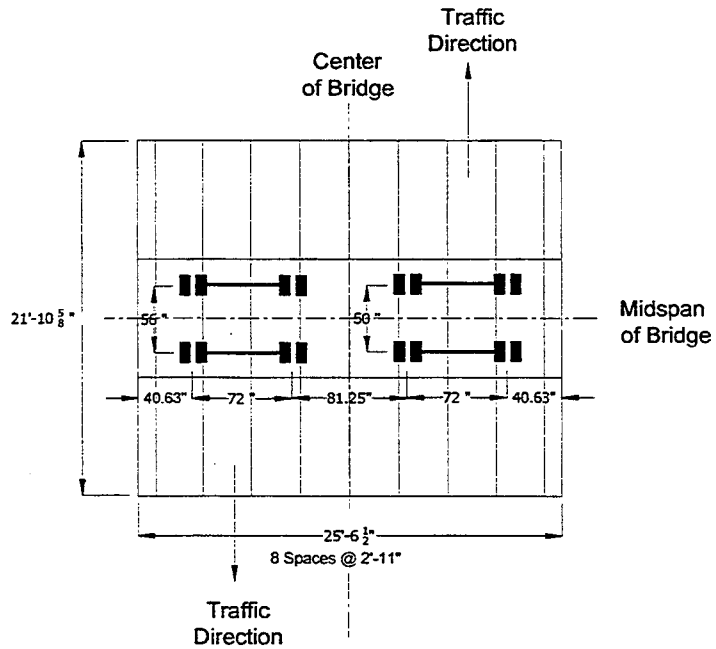


Figure 7. Position of Trucks on Each Lane.

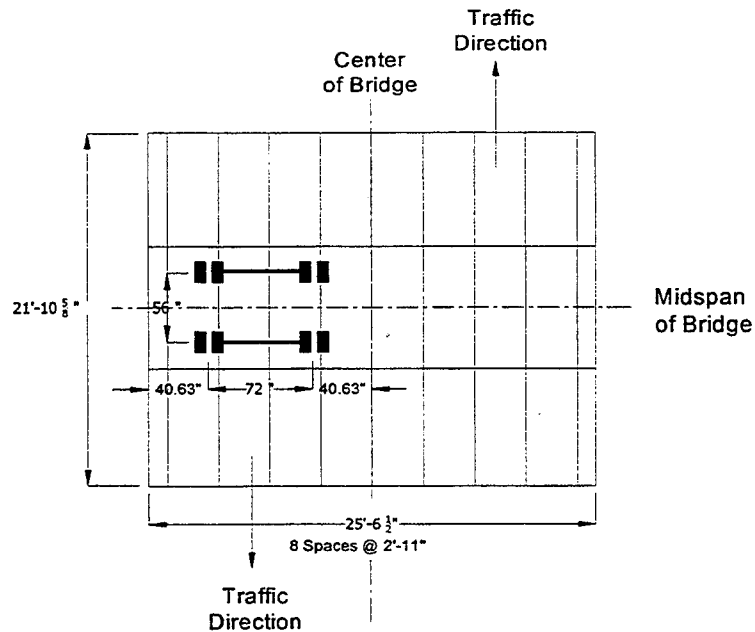


Figure 8. Position of Truck on One Lane Under Extreme Location – Close to Curb.

4.0 INSTRUMENTATION

Strains and deflections were measured at various locations of the deck and stringers. Strain gages were bonded to half of the steel stringers. Two gages were mounted on each stringer, one on the bottom of the top flange at mid-span of each stringer and the second gage on the top of the bottom flange of each stringer.

The FRP composite deck consisted totally of three panels, in which 10 strain gages were mounted at bottom flange of the FRP composite deck at location A (i.e., partially between Panel 1 and 2) and 10 strain gages at location B (i.e., at mid-span of panel 2).

The locations of strain gages are shown in figure 9.

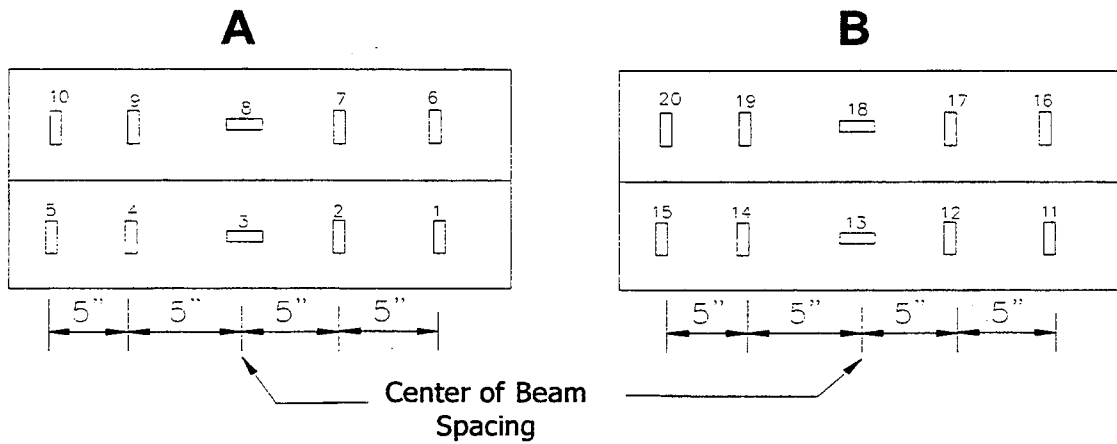
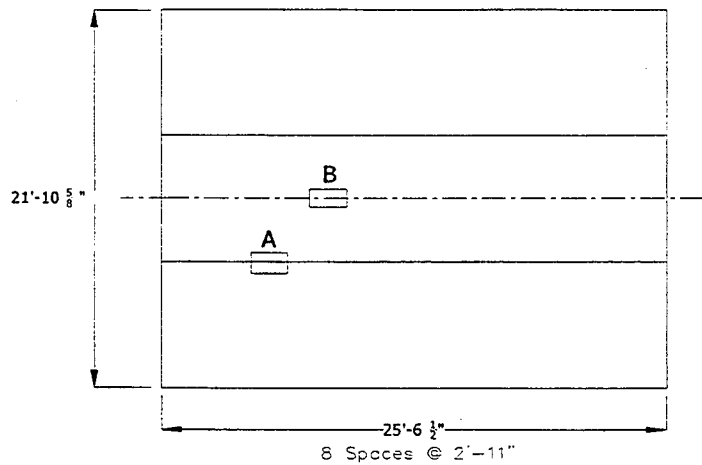


Figure 9. Location of Strain Gages on the Deck.

Deflections in the stringers were measured using a ruler and a theodolite. A steel ruler was mounted at mid-span of each stringer to measure deflections in the wide flange steel stringers under static loads. A theodolite mounted on the leveling staff was used to measure the variation of readings in the steel ruler.

5.0 LOAD TEST RESULTS

The strain and deflections data obtained from the three-load test were analyzed to:

- 1) Study the degree of structural composite action between the deck and supporting stringers.
- 2) Establish transverse load distribution factors for computing design moments for stringers.
- 3) Measure changes in bridge performance over a three-year period.
- 4) Evaluate fatigue behavior of deck-to-beam connections.

5.1 Degree of Structural Composite Action

The degree of compositeness is the ratio of the in-plane displacement due to bending at the plate-beam interface between the cases of partial and full composite action (Lopez, 1995). In the field, using the measured strain readings under static truckloads, the degree of structural compositeness between the deck and the steel stringers is established. Strains measured on the bottom of FRP deck, bottom of top flange of steel stringer, and bottom flange of stringer are used in the computation of degree of structural compositeness between the FRP deck and the stringers. Figure 10 illustrates the strain distribution through the depth of steel stringers for a typical load test. From the similar triangles, neutral axis is located at 7.99-in from the bottom of the stringers. The strain at the interface of the deck and the stringer, based on the neutral axis depth of 7.99-in is calculated to be 36 microstrains. Comparing the calculated value of 36 microstrains with the measured value of 27 microstrains at the interface of the FRP deck and stringer reveals a degree of structural compositeness between the FRP deck and stringer, which is about 75 percent. The high degree of compositeness, i.e., 75 percent is attributed to close spacing (35") of the steel stringers in the bridge superstructure.

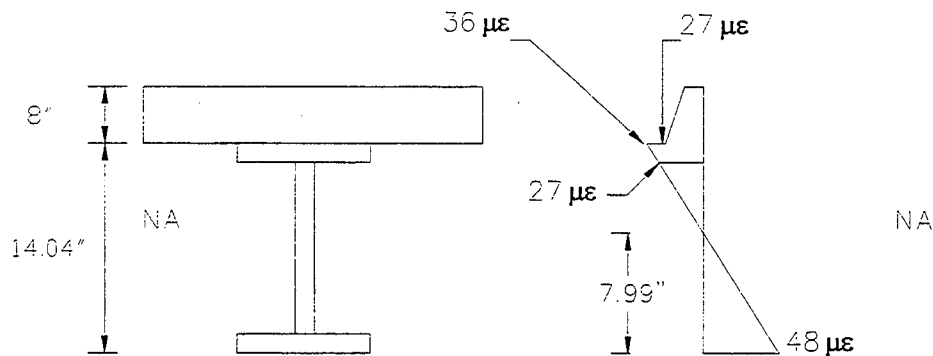


Figure 10. Typical Strain Distributions Through the Depth of Superstructure for a Stringer.

5.2 Transverse Load Distribution Factors

In an FRP composite deck system, the stiffening steel stringer is isolated from the rest of the structure and is subjected to a fraction of the applied load. This fraction that measures the load resistance at a given stringer location versus the resistance over the entire width in the transverse direction is called the transverse load distribution factor (TLDF) (Lopez, 1995).

The transverse load distribution factor is evaluated based on the strain of the stringers. Table 1 shows the maximum theoretical and experimental transverse distribution factors for LC1, LC2, and LC3 during three-year load tests. In the case of experimental test results, the maximum measured strain in the stringers (at mid-span) is divided by summation of peak strains in the remaining stringers to obtain transverse load distribution factors. In the case of theoretical evaluation of transverse load distribution factor, a first term approximation of Fourier series in macro-approach solution of orthotropic stiffened plates (Raju, 1989) is used. The equations and computation for TLDF are provided in the appendix A.

Load Test		LC1	LC2	LC3
1998	Experimental	0.26	0.12	0.26
	Theoretical	0.24	0.17	0.24
2000	Experimental	0.26	0.12	0.26
	Theoretical	0.24	0.17	0.24
2001	Experimental	0.26	0.12	0.26
	Theoretical	0.24	0.17	0.24

Table 1. Comparison of Theoretical and Experimental Transverse Load Distribution Factors.

Table 1 demonstrates good correlation between theoretical and experimental values for all load cases. When one fully loaded truck is placed on one lane (LC1 or LC3), the maximum transverse load distribution factor is found to be 0.26. The maximum axle load distribution factor

of 0.26 (in the case of LC1/LC3) translates to wheel load distribution factor of $\frac{S}{5.6}$. It compares

well with current AASHTO, 1994 equations ($\frac{S}{5.5}$) for two lanes or more.

5.3 Bridge Performance

Deflections and strains obtained from the load tests over a three-year period are used to evaluate the performance of Laurel Hill Creek Bridge. Measured strains and deflections in the field are compared with theoretical results. The experimental strain and deflection data are shown in appendix B. The theoretical evaluation of deflections and strains (appendix A) are based on first term approximation of the Fourier series in macro-approach solution of the orthotropic stiffened plates (Raju, 1989).

Table 2 shows deflection and strain values of the center stringer under static load tests over a three-year period. In the case of deflections, we observed a good co-relation between the experimental and theoretical test results. There is about 10 percent variation in deflections over a three-year period because the truckloads that were used in three-year period had about a 10 percent difference in magnitude. In the case of strains, under LC1 and LC3 i.e., when one truck is positioned on one lane, a certain kind of correlation is observed between the experimental and theoretical test results, while that for LC2 i.e., when one truck is positioned on each lane, the experimental and theoretical strains (not deflections) are varying by about 40 percent. Such variation is attributed to the fact that the theoretical equations are based only on pure flexure and are not coupled with flexure in combination with membrane effect. Moreover, the macro-approach solution for orthotropic plates is developed based on first term approximation, which is one of the reasons for the 40 percent difference in the experimental and theoretical strain values. As in the case of deflections, variation in strain over a three-year period was found to be about a 10 percent difference in magnitude of which is attributed to variation in magnitude of truckloads. This indicates that (over a three-year time period) there is no degradation in the superstructure including mechanical joints and chemical bonding.

Load Cases	Total Truck Load (ksi)	Deflections		Strains	
		Experimental	Theoretical	Experimental	Theoretical
1998					
LC1	60.8	0.031	0.042	41	48.1
LC2	119.3	0.094	0.082	52 *	92.5
LC3	58.5	0.031	0.039	41	44.4
2000					
LC1	50.3	0.025	0.035	33	39.5
LC2	105.5	0.084	0.078	46 *	87.9
LC3	55.2	0.025	0.035	40	39.5
2001					
LC1	51.5	0.025	0.037	33	41.6
LC2	107.3	0.083	0.078	46 *	86.9
LC3	51.5	0.025	0.035	35	39.6

Table 2. Comparison of Theoretical and Experimental Deflections and Strains.

*All three-load cases were evaluated for two trucks on the deck. The difference between the experimental and theoretical results is attributed to the spacing between two contiguous stringers, which is 35". It should be noted that the distance between the two truck tiers is assumed to be 4', while it is even larger than that in the field. Hence, field measurements are slightly underestimating the theoretical with theoretical values.

5.4 Deck Deformations

Since the spacing of stringers in Laurel Hill Creek Bridge is very close to (35"), it was difficult to measure the deck deformations. This is especially true when clear spacing of the FRP deck between the flanges of steel wide flange beams is 25".

5.5 Deck-to-Beam Connections

The deck was connected to the stringers by both mechanical fasteners and adhesive bonding. The fatigue of the joints between the deck and stringer is evaluated by computing the degree of compositeness (as shown in section 5.1) over a three-year period. It is found that degree of compositeness remained same (about 75 percent) during the three static load tests that were conducted in the years 1998, 2000, and 2001. These results indicate that there is no fatigue deterioration in the deck-to-beam connections.

6.0 CONCLUSIONS

In summer 1998, the FRP deck was installed on Laurel Hill Creek Bridge in Somerset County, Pennsylvania. The bridge was load tested in the fall of 1998, 2000, and 2001 to evaluate the performance of GFRP deck on steel stringers. The bridge was instrumented to measure strains and deflections under static loads. The following conclusions are drawn from the analysis of test results:

- The degree of compositeness between the FRP deck and steel stringer is about 75 percent.
- The TLDF is found to be $\frac{S}{5.6}$, which is close to the AASHTO equations.

- The variation in deflections and strains over three-year period indicates that there is no degradation in the system.
- There is no fatigue deterioration in the deck-to-stringer connections.

7.0 RECOMMENDATION

It is recommended to reinforce all the field joints in the FRP bridge deck with glass fabrics or any other equivalent material to prevent any cracking of wearing surface.

8.0 REFERENCES

GangaRao H.V.S., et.al., "Development of Glass Fiber Reinforced Polymer Composite Bridge Deck," SAMPE Journal, July/August 1999, pp 12-23.

GangaRao H.V.S., Witt J., Thippeswamy H., Justice J., "FRP Modular Bridge Deck Construction Issues," –Personnel Correspondence.

Nikki Overby, "Analysis and Design of Modular FRP Composite Bridge Deck," Masters Thesis, Department of Civil and Environmental Engineering, West Virginia University, Morgantown, West Virginia, 1998.

Raju, P.R. and Gangarao H.V.S., "Wheel Load Distribution on Highway Bridges," CFC Report No. 89-100, 98p, Constructed Facilities Center, West Virginia University.

Roberto Lopez-Anido, Dustin L. Troutman and John P. Busel. Fabrication and Installation of Modular FRP Composite Bridge Deck, Proceedings of International Composites Expo '98, Nashville, Tennessee, 1998, pp. 4-A/1 to 4-A/6.

Roberto Lopez-Anido," Analysis and Design of Orthotropic Plates Stiffened by Laminated Beams for Bridge Superstructures," Dissertation, Department of Civil and Environmental Engineering, West Virginia University, Morgantown, WV, 1995.

APPENDIX A

COMPUTATION PROCEDURES



APPENDIX A

COMPUTATION PROCEDURES

1. DISTRIBUTION LOAD FACTOR

Step 1. Compute the deck properties such as flexural rigidity, torsional rigidity of deck and flexural rigidity of stringer and the aspect ratio as shown in the following equations.

$$D_x = E_x I_x$$

$$D_y = E_y I_y$$

$$H = \sqrt{D_x D_y}$$

$$B_e = E_s I_s$$

$$\gamma = \frac{b}{a}$$

where

D_x = Flexural Rigidity of Deck in the x direction

D_y = Flexural Rigidity of Deck in the y direction

H = Torsional Rigidity of Deck

B_e = Flexural Rigidity of the Stringer

γ = The Aspect Ratio

E_x = Young's Modulus of the Deck in x Direction

E_y = Young's Modulus of the Deck in y Direction

E_s = Young's Modulus of the Stringer

I_x = Moment of Inertia of the Deck in x Direction

I_y = Moment of Inertia of the Deck in y Direction

I_s = Moment of Inertia of the Composite or Non-composite Stringer as the Case

b = Center to Center Distance Between the two External Stringers

a = Effective Span Length of the Bridge

Step 2. Compute the Equivalent Load

$$\text{Symmetric Load, } q_{11} = \frac{8P_e}{ab} \sin\left(\frac{\pi\xi}{a}\right) \sin\left(\frac{\pi\eta}{b}\right)$$

$$\text{Symmetric Load, } q_{12} = \frac{8P_e}{ab} \sin\left(\frac{\pi\xi}{a}\right) \sin\left(\frac{2\pi\eta}{b}\right)$$

where

P_e = Wheel Load of Each Truck Wheel

ξ = Location of the Wheel Load in y Direction

η = Location of the Wheel Load in x Direction

Step 3 Find Edge Deflection Coefficients C_0 and C_1

$$\text{Symmetric Load, } C_0 = \beta(2\gamma^2 + 1)$$

$$\text{Antisymmetric Load, } C_1 = \frac{4\beta(2 + \gamma^2)}{\left(1 + \frac{4\beta\gamma^2}{\pi}\right)}$$

$$\text{where } \beta = \left(\frac{b}{\pi}\right) \left(\frac{D_y}{B_e \gamma^4}\right)$$

Step 4. Find the overall flexural rigidity

$$\text{Symmetric Load, } D_{\text{Sym}} = D_y + 2H\gamma^2 + D_x \left(1 + \frac{4}{\pi} C_0\right) \gamma^4$$

$$\text{Antisymmetric Load, } D_{\text{Antisym}} = D_y + 2H \left(\frac{\gamma}{2}\right)^2 + D_x \left(1 + \frac{2}{\pi} C_1\right) \left(\frac{\gamma}{2}\right)^4$$

Step 5. Find the interactive forces R_{11} and R_{12} of the stringer for symmetric and antisymmetric load cases respectively.

$$\text{Symmetric Load, } R_{11} = \frac{bq_{11}}{\frac{D_{Sym}b}{B_e\gamma^4} + n\left(1 + \frac{4C_0}{\pi}\right)}$$

$$\text{Antisymmetric Load, } R_{12} = \frac{bq_{12}}{\frac{16D_{Antisym}b}{B_e\gamma^4} + n\left(1 + \frac{4C_1}{\pi}\right)}$$

Step 6. Find the idealized interactive force of the stringers supporting the deck $R(x, r)$ by summing the idealized interactive forces $R_{Sym}(x, r)$ and $R_{Antisym}(x, r)$ of symmetric and antisymmetric load cases.

$$R(x, r) = R_{Sym}(x, r) + R_{Antisym}(x, r)$$

$$R_{Sym}(x, r) = R_{11} \sin\left(\frac{\pi x}{a}\right) \sin\left(\frac{\pi r}{n} + C_0\right)$$

$$R_{Antisym}(x, r) = R_{12} \sin\left(\frac{\pi x}{a}\right) \left(\sin\left(\frac{2\pi r}{n}\right) + \left(1 - 2\frac{r}{n}\right)C_1 \right)$$

Step 7 Find the transverse load distribution factor of a stringer for applied forces. The transverse distribution factor (TLDF) is the ratio of the idealized interactive forces of a stringer to the sum of idealized interactive forces of all stringer.

$$\text{TLDF} = \frac{R(x, r)}{\sum_{r=0}^n R(x, r)}$$

where n is the total number of all stringers

2. DEFLECTION OF STRINGER

Symmetric Load,
$$w_{Sym}^R(x, r) = \frac{R_{11}}{B_e} \left(\frac{a}{\pi}\right)^4 \sin\left(\frac{\pi x}{a}\right) \left(\sin\left(\frac{\pi r}{n}\right) + C_0\right)$$

Antisymmetric Load,
$$w_{Antisym}^R(x, r) = \frac{R_{12}}{B_e} \left(\frac{a}{\pi}\right)^4 \sin\left(\frac{\pi x}{a}\right) \left(\sin\left(\frac{2\pi r}{n}\right) + C_1\left(1 - \frac{2r}{n}\right)\right)$$

Asymmetric Load,
$$w_{Asym}^R(x, r) = w_{Sym}^R(x, r) + w_{Antisym}^R(x, r)$$

Note All variables in above equations can be obtained from step 1 to step 6 in section 1.

3. STRAIN ON THE BOTTOM FLANGE OF STRINGERS

Step 1 Determine the interactive force on each stringer ($R(x, r)$) from step 6 in section 1. The

general form of $R(x, r)$ is $A_1 \sin\left(\frac{\pi x}{a}\right)$. A_1 is the amplitude of sine load acting on each stringer.

Step 2 Determine the Shear Force

$$V(x) = A_1 \left(\frac{a}{\pi}\right) \cos\left(\frac{\pi x}{a}\right)$$

Step 3 Determine the Moment

$$M(x) = A_1 \left(\frac{a}{\pi}\right)^2 \sin\left(\frac{\pi x}{a}\right)$$

Step 4 Determine the Bending Stress on the Bottom Flange of Stringers

$$\sigma_b = \frac{MC}{I_s}$$

Step 5 Determine the Strain on the Bottom Flange of Stringers

$$\varepsilon_b = \frac{\sigma_b}{E_s}$$

MATLAB CODES

All computations from section 1,2 and 3 will be coded in Matlab program as shown in the following pages in order to reduce the calculation time for the total of 9 load test over three year period.

1. DISTRIBUTION LOAD FACTOR

1.1 Matlab Code for Distribution Load Factor

```
clear
format compact
%Edeck_strong axis = 3.2e6
%Edeck_weak axis = 0.8e6
%Given Value
syms x
b = 23*12+4 % Width of Bridge (in)
a = 21*12+10.625 % Length of Bridge (in)
p = [0 0 23000 22800] % Individual Wheel Load (lbs)
Vx = 0.0625 %Vx is calculated from the ratio of Edeck times Vy
Vy = 0.25 %Vy means Vyx, Poisson Ratio when stress applied in y direction
Gamma = b/a
n = 8 % number of spacing
Dx = 1.82e7
Dy = 6.76e7
Dss = 4.49e6/12
Dxy = Vy*Dx
H = Dxy + 2*Dss
%H = Vx*Dy + Vy*Dx
Be = 29e6*899.89
psi = 12*[0 0 7.05 7.05]
nita = 12*[0 0 13.67 19.67]
P = p/2

%-----%

q11 = 4*P/a/b.*sin(pi*psi/a).*sin(pi*nita/b)
q12 = 4*P/a/b.*sin(pi*psi/a).*sin(2*pi*nita/b)
C0 = b*Dy/pi/Be*((1+(Vx+4*Dxy/Dy)*Gamma^2)/Gamma^4)
C1 =
(1+(4*Dxy/Dy+Vx)*Gamma^2/4)/(Be*Gamma^4*pi/Dy/8/b+(4*Dxy/Dy+Vx)*Gamma^2/4/pi)
Ds = Dx*Gamma^4*(1+4*C0/pi)+2*H*Gamma^2+Dy
Das = Dx*Gamma^4/16*(1+2*C1/pi)+2*H*Gamma^2/4+Dy
R11 = q11/(Ds/Gamma^4/Be+n/b*(1+4*C0/pi))
R12 = q12/(16*Das/Gamma^4/Be+n/b*(1+2*C1/pi))
r = 0:n
```

```

Rx_r_sym = vpa(R11*sin(pi*x/a)*(sin(pi*r/n)+C0),5)
Rx_r_antisym = vpa(R12*sin(pi*x/a)*(sin(2*pi*r/n)+C1*(1-2*r/n)),5)
Rx_r = vpa(Rx_r_sym + Rx_r_antisym,5)
Rx_r_final = sum(Rx_r)
DF = vpa(Rx_r_final/sum(Rx_r_final),5)
Sum_DF = sum(DF)

```

1.2 Results for Distribution Load Factor of Load Case 1 in 1998

To get started, select "MATLAB Help" from the Help menu.

```

b =
  280
a =
  262.6250
p =
   0   0  23000  22800
Vx =
  0.0625
Vy =
  0.2500
Gamma =
  1.0662
n = 8
Dx =
  18200000
Dy =
  67600000
Dss =
  3.7417e+005
Dxy =
  4550000
H =
  5.2983e+006
Be =
  2.6097e+010
psi =
   0   0  84.6000  84.6000
nita =
   0   0  164.0400  236.0400

```

```

P =
    0      0  11500  11400
q11 =
    0      0  0.5112  0.2489
q12 =
    0      0 -0.2725 -0.4386
C0 =
    0.2461
C1 =
    1.4999
Ds =
    1.1053e+008
Das =
    7.3484e+007
R11 =
    0      0  12.5299  6.1016
R12 =
    0      0 -3.0032 -4.8340
r =
    0  1  2  3  4  5  6  7  8
Rx_r_sym =
[      0,      0,      0,      0,      0,
0,      0,      0,      0]
[      0,      0,      0,      0,
0,      0,      0,      0]
[ 3.0831*sin(.11962e-1*x), 7.8781*sin(.11962e-1*x), 11.943*sin(.11962e-1*x),
14.659*sin(.11962e-1*x), 15.613*sin(.11962e-1*x), 14.659*sin(.11962e-1*x),
11.943*sin(.11962e-1*x), 7.8781*sin(.11962e-1*x), 3.0831*sin(.11962e-1*x)]
[ 1.5014*sin(.11962e-1*x), 3.8363*sin(.11962e-1*x), 5.8158*sin(.11962e-1*x),
7.1385*sin(.11962e-1*x), 7.6030*sin(.11962e-1*x), 7.1385*sin(.11962e-1*x),
5.8158*sin(.11962e-1*x), 3.8363*sin(.11962e-1*x), 1.5014*sin(.11962e-1*x)]
Rx_r_antisym =
[      0,      0,      0,      0,
0,      0,      0,      0]
[      0,      0,      0,      0,
0,      0,      0,      0]
[ -4.5044*sin(.11962e-1*x), -5.5018*sin(.11962e-1*x), -5.2554*sin(.11962e-1*x), -
3.2497*sin(.11962e-1*x), -.36778e-15*sin(.11962e-1*x), 3.2497*sin(.11962e-1*x),
5.2554*sin(.11962e-1*x), 5.5018*sin(.11962e-1*x), 4.5044*sin(.11962e-1*x)]
[ -7.2504*sin(.11962e-1*x), -8.8560*sin(.11962e-1*x), -8.4592*sin(.11962e-1*x), -
5.2308*sin(.11962e-1*x), -.59200e-15*sin(.11962e-1*x), 5.2308*sin(.11962e-1*x),
8.4592*sin(.11962e-1*x), 8.8560*sin(.11962e-1*x), 7.2504*sin(.11962e-1*x)]
Rx_r =

```

```

[      0,      0,      0,      0,      0,
0,      0,      0,      0]
[      0,      0,      0,      0,
0,      0,      0,      0]
[-1.4213*sin(.11962e-1*x), 2.3763*sin(.11962e-1*x), 6.6876*sin(.11962e-1*x),
11.409*sin(.11962e-1*x), 15.613*sin(.11962e-1*x), 17.909*sin(.11962e-1*x),
17.198*sin(.11962e-1*x), 13.380*sin(.11962e-1*x), 7.5875*sin(.11962e-1*x)]
[-5.7490*sin(.11962e-1*x), -5.0197*sin(.11962e-1*x), -2.6434*sin(.11962e-1*x),
1.9077*sin(.11962e-1*x), 7.6030*sin(.11962e-1*x), 12.369*sin(.11962e-1*x),
14.275*sin(.11962e-1*x), 12.692*sin(.11962e-1*x), 8.7518*sin(.11962e-1*x)]
Rx_r_final =
[-7.1703*sin(.11962e-1*x), -2.6434*sin(.11962e-1*x), 4.0442*sin(.11962e-1*x),
13.3167*sin(.11962e-1*x), 23.2160*sin(.11962e-1*x), 30.278*sin(.11962e-1*x),
31.473*sin(.11962e-1*x), 26.072*sin(.11962e-1*x), 16.3393*sin(.11962e-1*x)]
DF =
[-.53143e-1, -.19592e-1, .29974e-1, .98697e-1, .17207, .22441, .23326, .19323,
.12110]
Sum_DF =
1.000006
>>

```

2. DEFLECTION OF STRINGER

2.1 Matlab Codes for Deflection of Stringer

```

clear
format compact
%Edeck_strong axis = 3.2e6
%Edeck_weak axis = 0.8e6

%-----%
% Given Value
%-----%

syms x
b = 23*12+4 % Width of Bridge (in)
a = 21*12+10.625 % Length of Bridge (in)
p = [0 0 23000 22800] % Individual Wheel Load (lbs)
Vx = 0.0625 %Vx is calculated from the ratio of Edeck times Vy
Vy = 0.25 %Vy means Vyx, Poisson Ratio when stress applied in y direction
Gamma = b/a
n = 8 % number of spacing
Dx = 1.82e

```

```

Dy = 6.76e7
Dss = 4.49e6/12
Dxy = Vy*Dx
H = Dxy + 2*Dss
Be = 29e6*924.59
psi = 12*[0 0 7.05 7.05]
nita = 12*[0 0 13.67 19.67]
P = p/2

```

```

%-----%
% Calculation of Variables
%-----%

```

```

q11 = 4*P/a/b.*sin(pi*psi/a).*sin(pi*nita/b)
q12 = 4*P/a/b.*sin(pi*psi/a).*sin(2*pi*nita/b)
C0 = b*Dy/pi/Be*((1+(Vx+4*Dxy/Dy)*Gamma^2)/Gamma^4)
C1 =
(1+(4*Dxy/Dy+Vx)*Gamma^2/4)/(Be*Gamma^4*pi/Dy/8/b+(4*Dxy/Dy+Vx)*Gamma^2/4/pi)
Ds = Dx*Gamma^4*(1+4*C0/pi)+2*H*Gamma^2+Dy
Das = Dx*Gamma^4/16*(1+2*C1/pi)+2*H*Gamma^2/4+Dy
R11 = q11/(Ds/Gamma^4/Be+n/b*(1+4*C0/pi))
R12 = q12/(16*Das/Gamma^4/Be+n/b*(1+2*C1/pi))
A11 = R11/Be*(a/pi)^4
A12 = R12/Be*(a/pi)^4

```

```

%-----%
% Stringer Deflection at midspan of center beam
%-----%

```

```

r = 4 % r = 4 for the middle stringer ( r = 0,1,2,...,n)
wr_r_sym = A11*sin(pi/2)*(sin(pi*r/n)+C0) % x = a/2 for midspan deflection
wr_r_antisym = A12*sin(pi/2)*(sin(2*pi*r/n)+C1*(1-2*r/n)) % x = a/2 for midspan deflection
wr_r = wr_r_sym + wr_r_antisym
wr_r_final = sum(wr_r)

```

2.2 Results for Deflection of Center Stringer for Load Case 1 in 1998

b =
280
a =
262.6250
p =
0 0 23000 22800
Vx =
0.0625
Vy =
0.2500
Gamma =
1.0662
n =
8
Dx =
18200000
Dy =
67600000
Dss =
3.7417e+005
Dxy =
4550000
H =
5.2983e+006
Be =
2.6813e+010
psi =
0 0 84.6000 84.6000
nita =
0 0 164.0400 236.0400
P =
0 0 11500 11400
q11 =
0 0 0.5112 0.2489
q12 =
0 0 -0.2725 -0.4386
C0 =
0.2395
C1 =
1.4614
Ds =
1.1033e+008
Das =
7.3448e+007

```

R11 =
    0    0 12.6328  6.1517
R12 =
    0    0 -3.0587 -4.9235
A11 =
    0    0 0.0230  0.0112
A12 =
    0    0 -0.0056 -0.0090
r =
    4
wr_r_sym =
    0    0 0.0285  0.0139
wr_r_antisym =
1.0e-017 *
    0    0 -0.0682 -0.1098
wr_r =
    0    0 0.0285  0.0139
wr_r_final =
    0.0424
>>

```

3. STRAIN ON THE BOTTOM FLANGE OF STRINGER

3.1 Matlab Codes for Strain on the Bottom Flange of Stringer

```

clear
format compact
%Edeck_strong axis = 3.2e6
%Edeck_weak axis = 0.8e6

%-----%
% Given Value
%-----%

syms x
b = 23*12+4 % Width of Bridge (in)
a = 21*12+10.625 % Length of Bridge (in)
p = [0 0 23000 22800] % Individual Wheel Load (lbs)
Vx = 0.0625 %Vx is calculated from the ratio of Edeck times Vy
Vy = 0.25 %Vy means Vyx, Poisson Ratio when stress applied in y direction
Gamma = b/a
n = 8 % number of spacing
Dx = 1.82e7
Dy = 6.76e7
Dss = 4.49e6/1

```

$$D_{xy} = V_y \cdot D_x$$

$$H = D_{xy} + 2 \cdot D_{ss}$$

$$B_e = 29e6 \cdot 924.59$$

$$\psi = 12 \cdot [0 \ 0 \ 7.05 \ 7.05]$$

$$\eta = 12 \cdot [0 \ 0 \ 13.67 \ 19.67]$$

$$P = p/2$$

%-----%
% Calculation of Variables
%-----%

$$q_{11} = 4 \cdot P/a/b \cdot \sin(\pi \cdot \psi/a) \cdot \sin(\pi \cdot \eta/b)$$

$$q_{12} = 4 \cdot P/a/b \cdot \sin(\pi \cdot \psi/a) \cdot \sin(2 \cdot \pi \cdot \eta/b)$$

$$C_0 = b \cdot D_y/\pi/B_e \cdot ((1 + (V_x + 4 \cdot D_{xy}/D_y) \cdot \Gamma^2)/\Gamma^4)$$

$$C_1 =$$

$$(1 + (4 \cdot D_{xy}/D_y + V_x) \cdot \Gamma^2/4) / (B_e \cdot \Gamma^4 \cdot \pi/D_y/8/b + (4 \cdot D_{xy}/D_y + V_x) \cdot \Gamma^2/4/\pi)$$

$$D_s = D_x \cdot \Gamma^4 \cdot (1 + 4 \cdot C_0/\pi) + 2 \cdot H \cdot \Gamma^2 + D_y$$

$$D_{as} = D_x \cdot \Gamma^4/16 \cdot (1 + 2 \cdot C_1/\pi) + 2 \cdot H \cdot \Gamma^2/4 + D_y$$

$$R_{11} = q_{11}/(D_s/\Gamma^4/B_e + \eta/b \cdot (1 + 4 \cdot C_0/\pi))$$

$$R_{12} = q_{12}/(16 \cdot D_{as}/\Gamma^4/B_e + \eta/b \cdot (1 + 2 \cdot C_1/\pi))$$

$$A_{11} = R_{11}/B_e \cdot (a/\pi)^4$$

$$A_{12} = R_{12}/B_e \cdot (a/\pi)^4$$

%-----%
% Interaction force at center beam
%-----%

$$r = 4 \quad \% r = 4 \text{ for the center stringer } (r = 0, 1, 2, \dots, n)$$

digits(4)

$$R_{r_sym} = vpa(R_{11} \cdot (\sin(\pi \cdot r/n) + C_0)) \cdot \sin(\pi \cdot x/a) \quad \% \text{ Interaction force for symmetric case}$$

$$R_{r_antisym} = vpa(R_{12} \cdot (\sin(2 \cdot \pi \cdot r/n) + C_1 \cdot (1 - 2 \cdot r/n))) \cdot \sin(\pi \cdot x/a) \quad \% \text{ Interaction force for antisymmetric case}$$

$$R_r = R_{r_sym} + R_{r_antisym}$$

$$R_{r_final} = \text{sum}(R_r) \quad \% \text{ Interaction force on the beam}$$

%-----%
% Shear and Moment at center beam
%-----%

$$E_{str} = 29e6$$

$$I_c = 924.59$$

$$\text{Shear} = \text{int}(-1 \cdot R_{r_final}, x) \quad \% \text{ Shear in beam}$$

$$\text{Moment} = \text{int}(\text{Shear}, x) \quad \% \text{ Moment in beam}$$

$$\text{Slope} = \text{int}(\text{Moment}, x)$$

Deflection = int(Slope,x)/(Estr*Ic)
 Def_center = subs(Deflection,x,a/2)
 Mcenter = subs(Moment,x,a/2) % Moment at midspan

%------%
 % Stress and Strain at midspan of center beam
 %------%

c = 7.92
 Stress = Mcenter*c/Ic % Stress Unit is psi.
 Strain = Stress/Estr*10^6 % Strain Unit is microstrian.

%------%
 % Back Calculate the Amplitude of sine curve from deflection
 %------%
 %y = 0.0836 % Theoretical Deflection
 %P = y*Estr*Ic*pi^4/a^4

3.2 Results of Strain on the Bottom Flange of Center Stringer for Load Case 1 in 1998

b =
 280
 a =
 262.6250
 p =
 0 0 23000 22800
 Vx =
 0.0625
 Vy =
 0.2500
 Gamma =
 1.0662
 n =
 8
 Dx =
 18200000
 Dy =
 67600000
 Dss =
 3.7417e+005
 Dxy =
 4550000
 H =
 5.2983e+006
 Be =
 2.6813e+010

```

psi =
  0    0 84.6000 84.6000
nita =
  0    0 164.0400 236.0400

P =
  0    0 11500 11400
q11 =
  0    0 0.5112 0.2489
q12 =
  0    0 -0.2725 -0.4386
C0 =
  0.2395
C1 =
  1.4614
Ds =
  1.1033e+008
Das = 7.3448e+007
R11 =
  0    0 12.6328 6.1517
R12 =
  0    0 -3.0587 -4.9235
A11 =
  0    0 0.0230 0.0112
A12 =
  0    0 -0.0056 -0.0090
r =
  4
R_r_sym =
[      0,      0, 15.66*sin(8/2101*pi*x), 7.625*sin(8/2101*pi*x)]
R_r_antisym =
[      0,      0, -3.746e-15*sin(8/2101*pi*x), -.6029e-
15*sin(8/2101*pi*x)]
R_r =
[      0,      0, 15.66*sin(8/2101*pi*x), 7.625*sin(8/2101*pi*x)]

R_r_final =
23.29*sin(8/2101*pi*x)
Estr =
  29000000
Ic =
  924.5900
Shear =
1947.*cos(.1196e-1*x)
Moment =.1628e6*sin(.1196e-1*x)

```

Slope =
-.1361e8*cos(.1196e-1*x)
Deflection =
-.4244e-1*sin(.1196e-1*x)
Def_center =
-0.0424
Mcenter =
1.6280e+005
c =
7.9200
Stress =
1.3945e+003
Strain =
48.0875
>>



APPENDIX B



APPENDIX B

October 29, 1998

Strain Gage Data (Microstrain)

Gage No.	LC1	LC2	LC3
1	-15	-44	20
2	-13	14	26
3	0	-27	-32
4	-8	23	30
5	-5	18	25
6	-3	28	34
7	-7	24	29
8	2	-30	-37
9	-10	22	30
10	-4	19	21
11	-10	40	37
12	-21	30	24
13	-11	-38	-48
14	-10	39	39
15	-8	44	45
16	2	47	38
17	-9	36	28
18	3	-23	-37
19	-12	33	33
20	-7	39	37
S1	-2	28	30
	-6	-63	-62
S2	1	42	42
	-10	-79	-74
S3	7	64	56
	-18	-73	-58
S4	19	48	21
	-15	-32	-17
S5	41	52	41
	-43	-85	-43
S6	21	48	19
	-17	-32	-15
S7	56	64	7
	-58	-73	-18
S8	42	42	1
	-74	-79	-10
S9	30	28	-2
	-62	-63	-6

Deflection Data (Inches)

Str. No.	LC1	LC2	LC3
S1	0.000	-0.063	-0.063
S2	0.000	-0.063	-0.094
S3	0.000	-0.094	-0.094
S4	-0.031	-0.094	-0.094
S5	-0.031	-0.094	-0.094
S6	-0.063	-0.125	-0.063
S7	-0.063	-0.094	0.000
S8	-0.063	-0.063	0.000
S9	-0.063	-0.063	0.000

December 15, 2000

Strain Data

Gage No.	LC1	LC2	LC3
1	-12	-39	20
2	-11	12	25
3	0	-24	-31
4	-6	21	29
5	-4	16	24
6	-2	25	33
7	-6	21	28
8	2	-27	-36
9	-8	20	29
10	-3	17	20
11	-8	36	36
12	-17	27	23
13	-9	-34	-47
14	-8	35	38
15	-6	39	44
16	2	42	37
17	-7	32	27
18	2	-21	-36
19	-10	29	32
20	-6	35	36
S1	-2	25	29
	-5	-56	-61
S2	1	37	41
	-8	-70	-72
S3	6	57	55
	-15	-65	-57
S4	15	43	20
	-12	-29	-17
S5	33	46	40
	-35	-76	-42
S6	17	43	19
	-14	-29	-15
S7	45	57	7
	-47	-65	-18
S8	34	37	1
	-60	-70	-10
S9	24	25	-2
	-51	-56	-6

Deflection Data

Str. No.	LC1	LC2	LC3
S1	0.000	-0.056	-0.061
S2	0.000	-0.056	-0.092
S3	0.000	-0.084	-0.092
S4	-0.025	-0.084	-0.092
S5	-0.025	-0.084	-0.092
S6	-0.051	-0.111	-0.061
S7	-0.051	-0.084	0.000
S8	-0.051	-0.056	0.000
S9	-0.051	-0.056	0.000

May 23 2001
Strain Data

Gage No.	LC1	LC2	LC3
1	-12	-39	17
2	-10	12	22
3	0	-24	-27
4	-6	20	26
5	-4	16	21
6	-2	25	29
7	-6	21	25
8	2	-26	-31
9	-8	19	26
10	-3	17	18
11	-8	35	31
12	-17	26	20
13	-9	-33	-41
14	-8	34	33
15	-6	39	38
16	2	41	32
17	-7	32	24
18	2	-20	-31
19	-10	29	28
20	-6	34	31
S1	-2	25	26
	-5	-55	-53
S2	1	37	36
	-8	-70	-63
S3	6	56	48
	-15	-64	-49
S4	15	42	18
	-12	-28	-14
S5	33	46	35
	-35	-75	-37
S6	17	42	16
	-14	-28	-13
S7	45	56	6
	-47	-64	-15
S8	34	37	1
	-60	-70	-9
S9	24	25	-2
	-50	-55	-5

Deflection Data

Str. No.	LC1 (36,900 lbs)	LC2 (78,525 lbs)	LC3 (36,900 lbs)
S1	0.000	-0.055	-0.054
S2	0.000	-0.055	-0.080
S3	0.000	-0.083	-0.080
S4	-0.025	-0.083	-0.080
S5	-0.025	-0.083	-0.080
S6	-0.051	-0.110	-0.054
S7	-0.051	-0.083	0.000
S8	-0.051	-0.055	0.000
S9	-0.051	-0.055	0.000